Front. Chem. Sci. Eng. 2021, 15(5): 1147–1157
https://doi.org/10.1007/s11705-020-1978-x

RESEARCH ARTICLE

Insight into the effect of surface carboxyl and amino groups on the adsorption of titanium dioxide for acid red G

Wenlong Zhang[1], Xuyang Zhao[1], Lin Zhang[1], Jinwei Zhu[1,2], Shanshan Li[1], Ping Hu[3], Jiangtao Feng (✉)[1], Wei Yan[1]

1 Department of Environmental Science and Engineering, Xi'an Jiaotong University, Xi'an 710049, China
2 Shaanxi Electrical Equipment Institution, Xi'an 710025, China
3 Shaanxi Polytechnic Institute, Xianyang 712000, China

Abstract In this study, TiO_2 functionalized with organic groups were prepared to study the effect of carboxyl and amino groups on the adsorption behavior of TiO_2 for the removal of acid red G (ARG) as an anionic dye from aqueous solution. TiO_2 was successfully modified with carboxyl and amino groups by using the hydrolysis method with oxalic acid (OAD, with two carboxyl groups), ethylenediamine (EDA, with two amino groups) and DL-alanine (DLA, with one carboxyl group and one amino group) at low temperature (65 °C) and labeled as OAD-TiO_2, EDA-TiO_2 and DLA-TiO_2, respectively. The ARG uptake by the functionalized TiO_2 samples was largely dependent on the functional groups. The interaction between ARG and the functional organic groups on the TiO_2 samples plays an important role in the adsorption process, which leads to the excellent adsorption performance (higher capacity and faster adsorption rate) of the functionalized TiO_2 samples than that of P25 (commercial TiO_2 without modification). Furthermore, there is no obvious loss of the adsorption capacity for the functionalized TiO_2 even after 5 adsorption-desorption cycles, which indicated the good reusability of the modified TiO_2 samples for anionic dye removal from aqueous solution.

Keywords amino group, carboxylic group, titanium dioxide, ARG, adsorption

1 Introduction

TiO_2 is a remarkable photocatalyst and numerous researches about heterogeneous photocatalysis related to TiO_2 have been published [1–4]. Due to the excellent photochemical property, TiO_2 is also employed as a catalyst for the pollution removal from air or water [5–7]. Moreover, the adsorption ability of TiO_2 plays an important role in the effective photo degradation of organic matters, although TiO_2 is usually used as the photocatalyst [8]. The pristine TiO_2 has a limited adsorption capacity due to its intrinsic defects, such as low specific surface area and few surface active sites [9]. Meanwhile, the surface active sites are considered to be one of the most significant factors for the adsorption process [10]. Nowadays, an increasing number of studies focused on the approaches to enhance the adsorption property of TiO_2. Introducing the functional groups onto the TiO_2 surface, such as hydroxyl, carboxyl or amino groups, has been considered as one of the effective methods. In addition, the functional groups bring TiO_2 not only the enhanced adsorption capacity, but also an increased adsorption rate [11].

The introduction of hydroxyl, carboxyl or amino groups can change the surface charge and electron distribution of TiO_2 and influence the interactions between the adsorbates and the modified TiO_2. Therefore, the enhanced adsorption capacity of TiO_2 for organic and inorganic adsorbates could probably be achieved by the functionalization of the hydroxyl, carboxyl or amino groups [12,13]. It was reported that the carboxyl modification could be in favor of the cations adsorption [12]. On the contrary, the amino functionalization was propitious to the adsorption of the anions contaminants [13]. The surface functional groups like carboxyl and amino were usually introduced onto TiO_2 by two approaches. One is anchoring the relevant organic groups onto the surface of the as-prepared TiO_2 particles [14]. In this method, the modified TiO_2 was obtained at higher temperature to strengthen the binding force between the functional groups and TiO_2 structure. The other way is the *in-situ* synthesis [15], which is a reaction of titanium source (usually tetrabutyl titanate, isopropyl titanate or titanium chloride) and chemicals

Received April 19, 2020; accepted June 25, 2020

E-mail: fjtes@xjtu.edu.cn

containing functional groups [16]. The preferable functionalized TiO_2 is obtained by the latter facile method in one step hydrothermal process at lower temperature.

The carboxyl groups can be linked to TiO_2 with the bond formation of bridging, chelating and ester-like linkage [17,18]. Nguyen-Phan et al. [15] found that the carboxylate groups of succinic acid could be coordinated to TiO_2 in the form of bridging and chelating structure after calcined at 400 °C for 5 h. The maximum capacity of the modified TiO_2 for methylene blue (MB) was reported as 32.15 mg/g. The amino groups could be grafted on TiO_2 by the hydrogen bonding between NH_2 group and hydroxyl or carboxyl group on TiO_2 surface [19,20]. For instance, Sugita et al. [13] synthesized an amino functionalized TiO_2 with 3-[2-(2-aminoethylamino) ethylamino] propyl-trimethoxysilane and the modified sample exhibited more excellent adsorption capacity for indigo carmine than that of pristine TiO_2.

Based on the above information, we focus on the influence of carboxyl and amino groups on adsorption performance of TiO_2. The TiO_2 samples modified by the organic chemicals with carboxyl and/or amino groups were prepared at low temperature. ARG, one of the typical anionic dyes in wastewater which could cause severe pollution [21], was employed as the target contaminant to examine the effect of functional groups in the adsorption process. It is found that the carboxyl and amino functionalization significantly affect the adsorption behavior of the TiO_2 samples for anionic dye ARG.

2 Experimental

2.1 Materials

Tetrabutyl titanate (TBT, 340.36 g/mol, 98%), *n*-propanol (60.10 g/mol, 99%), oxalic acid (OAD, 90.04 g/mol, 99.5%), ethylenediamine (EDA, 60.10 g/mol, 99.0%) and DL-alanine (DLA, 89.09 g/mol, 98.5%) were of analytical grade and got from Sinopharm Chemical Reagent Co., Ltd., Shanghai, China. Anionic dye ARG (509.42 g/mol, 99.0%) was purchased from Beijing Chemical Reagent Co. of China and used as received. The deionized water used in this study was obtained from the EPED-40TF Superpure Water System (EPED, China).

2.2 Synthesis of functional TiO_2 samples

The functional TiO_2 samples were prepared by the one-step hydrolysis approach at a low temperature. A typical pathway was as follows: firstly, the organic compound (OAD, EDA or DLA) was dissolved into deionized water to form the 0.16 mol/L solution which was labeled as solution A. The mixture solution containing TBT and *n*-propanol (the volume ratio is 5:2) was also prepared and named solution B. Then, 14 mL solution B was slowly added into 200 mL solution A with magnetic stirring (300 r/min) for 2 h at 65 °C, the white suspension solution was formed. And the suspension was stirred for another 12 h at the ambient temperature. After that, the white solid was collected by filtration and rinsed with water until the pH value of the filtrate was neutral. The collected white solid was dried at 60 °C for 24 h. the as-prepared samples were labeled as OAD-TiO_2, EDA-TiO_2 or DLA-TiO_2 according to the organic compound added in the preparation process. The P25 from the Degussa was employed as the no-functional group comparator.

2.3 Analysis and characterization methods

Fourier Transform Infrared spectra (FTIR) of the samples were carried out on BRUKER TENSOR 37 FT-IR spectrophotometer in the range of 4000–400 cm^{-1} by the KBr pellet method. The morphology and elemental information were obtained on a scanning electron microscopy (SEM, JSM-6700F, Japan) with an energy dispersive X-ray spectroscopy (EDX). The thermogravimetric analysis (TG) was performed on a Setaram Labsys Evo in N_2 flow with the heating rate of 10 °C/min over a temperature within 30–800 °C. Zeta potentials were tested with NanoBrook 90Plus Analyzer. Samples for zeta potential measurement were prepared by adding 1 mg of TiO_2 into 10 mL NaCl solution (0.1 mmol/L) at different pH values from 2 to 12 (adjusted with 0.1 mol/L HNO_3 or NaOH solution). N_2 adsorption and desorption isotherms were recorded on a Builder SSA-4200 at 77 K. The specific surface area is calculated using the multiple point Brunner-Emmett-Teller (BET) method, and total pore volume and average pore radius were calculated based on the BJH (Barrett-Joyner-Halenda) method (using the desorption branch).

2.4 Adsorption experiments

The adsorption of ARG was carried out by shaking the mixture of solution with the modified TiO_2 samples (2.0 g/L) at 25 °C. Then the suspension was centrifuged at 4000 r/min for 5 min. The supernatant was analyzed by the UV-Vis spectrophotometer (Agilent 8453) and the absorbance value was read at the wavelength of 531 nm, in order to evaluate the adsorption capacity of ARG onto TiO_2 samples. The amount of ARG molecules adsorbed onto the TiO_2 samples Q_t (mg/g) at a certain time t was calculated from Eq. (1):

$$Q_t = \frac{C_0 - C_t}{m} \times V, \tag{1}$$

where C_0 (mg/L) and C_t (mg/L) are the initial concentration and residual concentration at time t (min) of the ARG solution, respectively; V (L) is the ARG solution volume, and m (g) is TiO_2 sample mass.

Adsorption kinetic experiments were carried out in a conical flask by contacting 0.1 g of the TiO_2 samples and 50 mL solution with certain concentration (100, 200, 300 mg/L in this study) of ARG solution at 25 °C. In various contact time from 0 to 120 min, 2 mL samples were withdrawn and filtered to evaluate the adsorption capacity of the TiO_2 samples. The pseudo-first order and pseudo-second order models (Eqs. (2) and (3)) were employed to fit the kinetic experiment data.

$$Q_t = Q_e(1 - e^{-K_1 t}), \tag{2}$$

$$Q_t = \frac{K_2 Q_e^2 t}{1 + K_2 Q_e t}, \tag{3}$$

where t is the adsorption time (min); K_1 (min^{-1}) and K_2 (g/(mg·min)) are the rate constants for the pseudo-first-order and pseudo-second-order models, respectively; Q_t and Q_e (mg/g) are the adsorption capacity at t min and equilibrium time, respectively.

The adsorption isotherms of ARG onto the TiO_2 samples were obtained by mixing different initial concentrations (10–500 mg/L) of ARG solution with 2 g/L of the TiO_2 samples, and then the solution was shaken for 120 min in dark at 25 °C. The Langmuir and Freundlich isotherm models were described according to Eqs. (4) and (5), respectively:

$$Q_t = \frac{Q_{max} K_L C_t}{1 + K_L C_t}, \tag{4}$$

$$Q_e = K_F C_e^{1/n}, \tag{5}$$

where Q_{max} (mg/g) is the maximum monolayer molecular adsorption capacity onto the adsorbent in Langmuir isotherm model; K_L (L/mg) and K_F ((mg/g)/(mg/L)^n) are the constant of Langmuir and Freundlich isotherm model, respectively. $1/n$ represents the degree of adsorption dependence on equilibrium concentration in Freundlich isotherm model. In addition, the dimensionless separation factor R_L, an essential characteristic of the Langmuir model to reflect the favorability of an adsorption process, is expressed as:

$$R_L = \frac{1}{1 + K_L C_m}, \tag{6}$$

where C_m (mg/L) is the maximum initial concentration of ARG in solution.

In the regeneration study, 200 mg/L ARG solution was being contacted with the TiO_2 sample for 120 min. Then, the exhausted TiO_2 sample was immersed in 0.1 mol/L NaOH solution for 20 min to release ARG from the TiO_2 sample, and further immersed in 0.1 mol/L HNO_3 solution to activate. The regenerated TiO_2 sample was again used as the adsorbent to remove ARG from the aqueous solution. And the adsorption capacity of the regenerated TiO_2 was recorded to evaluate the regeneration property of the functional TiO_2 samples and P25.

3 Results and discussion

3.1 Characterizations of TiO_2 samples

The FTIR spectra (Fig. 1) of P25 and the modified TiO_2 samples were analyzed to examine the existence of the functional groups. For P25, the wide peak between 900–400 cm^{-1} belongs to the Ti–O–Ti stretching vibration [22]. The other wide peak at 3600–3200 cm^{-1} is very weak and ascribed to the stretch of hydroxyl groups on the surface of TiO_2 (P25). The peaks for the copious groups in the functionalized TiO_2 samples appear in the FTIR spectra. The broad peak in the range of 3600–2500 cm^{-1} is attributed to the vibration of –OH in carboxylic group. The peaks for $–NH_2$ stretching vibration (3450–3220 cm^{-1}) and strong peak of –OH group are overlapped in this broad range of the spectra of EDA-TiO_2 and DLA-TiO_2. A broad and strong peak at 1690 cm^{-1} in the spectrum of OAD-TiO_2 is ascribed to the C = O stretching vibration of saturated dicarboxylic acid. The peaks at 1620 and 1430 cm^{-1} are related to the asymmetric and symmetric bending vibrations of COO^- group, respectively. The value of $\Delta\nu$ (COO^-) for the OAD-TiO_2 sample is approximate 190 cm^{-1}, which illustrates a bridging structure between OAD and TiO_2 [23–25]. The peak at 1288 cm^{-1} corresponds to the stretching vibration of C–O bond. While for the EDA-TiO_2 and DLA-TiO_2 samples, N–H bending vibration of primary amine are observed at around 1620 cm^{-1}. The peak at 1510 cm^{-1} (only for EDA-TiO_2, which is not found in the spectrum of DLA-TiO_2)is ascribed to the deformation vibration of N–H in the secondary amine, which indicates there is hydrogen

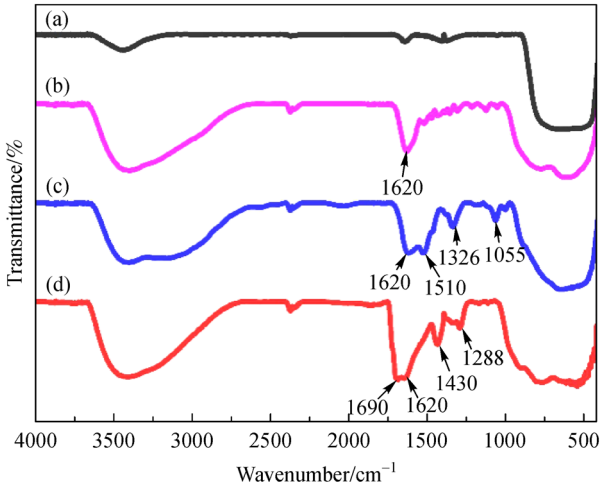

Fig. 1 FTIR spectra of (a) P25, (b) DLA-TiO_2, (c) EDA-TiO_2 and (d) OAD-TiO_2.

bonding between the amino group and TiO_2 [19]. The bond at 1326 cm^{-1} (for EDA-TiO_2) is assigned to the stretching vibration of C–N [26]. At the spectrum of DLA-TiO_2, the peak belonging to C = O disappears, which might be caused by the binding of the carboxyl in the DLA and the TiO_2 with chelation [23]. The analysis of FTIR results demonstrates the existence of carboxyl and amino groups and success of TiO_2 functionalization.

The morphologies of the TiO_2 samples are observed by SEM (Fig. S1 with EDX results, cf. Electronic Supplementary Material, ESM). The particle size of P25 is so small that the image is not so clear even the magnification is 10000 times. The functional TiO_2 samples are composed of the micro-particles. And the particle size of OAD-TiO_2 is significantly larger than that of EDA-TiO_2 and DLA-TiO_2. In addition, it is obvious that there are certain amounts of pore existing in the structure of EDA-TiO_2 and DLA-TiO_2. These results suggested that the difference of amino acid used in functional synthesis could cause effect on the morphology of the prepared materials. Furthermore, the group species and number contained in amino acid might be the main factor and amino groups are probably more beneficial to the porous and granular morphology than carboxy groups.

The surface content of each element was also obtained by EDX and listed in Table 1. The functionalization degree may be described by the atom molar C/Ti because C is primarily associated with organic matter in the samples. The C/Ti ratio for the functional TiO_2 samples (C/Ti = 0.137, 0.207 and 0.547 for OAD-TiO_2, EDA-TiO_2 and DLA-TiO_2, respectively) was much higher than that of P25 (C/Ti = 0.065), which suggests that these samples contain a great amount of organic residues. The above result indicates certain original organic structures were successfully introduced to these functional TiO_2, which is consistent with the results of FTIR spectra.

The TG results were also analyzed to prove the organic groups existence in the functional TiO_2 samples (Fig. 2). For the P25, there is no weight lost at all TG test temperature except for very little loss of adsorbed water. For all the functional TiO_2 samples, the first thermal degradation step losing of around 15.0 wt-% below 200 °C is attributed to the loss of adsorbed water. The second thermal degradation step after 200 °C is possibly ascribed to the decomposition of the organic groups on the TiO_2 samples [15]. For the OAD-TiO_2 and DLA-TiO_2, the second step is a simple and similar weight loss about 5.0 wt-%, however, the EDA-TiO_2 exhibits different weight loss (9.0 wt-%) at the same range of temperature (200–540 °C). The above results are attributed to the thermal decomposition of the organics from the hydrolysis of titanium (IV) butoxide precursor, carboxylic and hydroxyl groups on the functional TiO_2 surface. The weight loss results reveal the different organic contents in different samples. The weight loss step over 540 °C is considered as the loss of amino groups on the surface of EDA-TiO_2. The TG result indicates that there are several functional groups on the modified TiO_2 surface and the interaction between organic groups and TiO_2 in EDA-TiO_2 is different from that of OAD-TiO_2 and DLA-TiO_2, which is similar with the result of FTIR test.

The zeta potential of the modified TiO_2 samples under different solution pH is shown in Fig. 3. The isoelectric point (pH_{iep}) is the pH value of the solution when the zeta potential is zero. The pH_{iep} values of the functional TiO_2 samples decreased intensely after modified by carboxyl and amino groups. The OAD-TiO_2 sample exhibited lower pH_{iep} value than others. This can be deduced that the carboxyl group in OAD make its surface negatively charged easily. The TiO_2 samples are gradually more positively charged while the increasing number of amino groups were introduced into the functional TiO_2 samples like DLA-TiO_2 and EDA-TiO_2. In addition, the pH_{iep} of functionalized samples are all less than that of P25. The value of zeta potential of adsorbents materials should be focused on because this parameter could affect the interaction between TiO_2 samples and contaminants [27]. In fact, lower pH_{iep} for sample is not favorable to enhance the adsorption efficiency of anions such as ARG. Therefore, the adsorption capacity of modified TiO_2 will be compared with that of P25 in the "adsorption mechanism" to find the role of electrostatic attraction in the adsorption process.

The BET surface area (S_{BET}), pore volume (V_p) and pore diameter parameters of the TiO_2 samples are listed in Table 2. The S_{BET} and pore diameter were calculated from the corresponding nitrogen adsorption-desorption isotherms and the desorption branch of the nitrogen isotherms by the BJH (Fig. S2, cf. ESM). It can be seen from the data that the S_{BET} of the OAD-TiO_2 and EDA-TiO_2 are smaller than that of the P25, while the S_{BET} of the DLA-TiO_2 is larger than the value of P25. The phenomenon can be

Table 1 The surface molar ratio of different atoms for the TiO_2 samples

Sample	C/atom %	Ti/atom %	O/atom %	C/Ti
P25[a)]	4.19	63.69	32.12	0.065
OAD-TiO_2[b)]	8.18	59.90	28.57	0.137
EDA-TiO_2[c)]	11.93	57.61	30.47	0.207
DLA-TiO_2[d)]	24.68	45.09	30.23	0.547

a) P25: commercial bare TiO_2; b) OAD-TiO_2: oxalic acid modified TiO_2; c) EDA-TiO_2: ethylenediamine modified TiO_2; d) DLA-TiO_2: DL-alanine modified TiO_2.

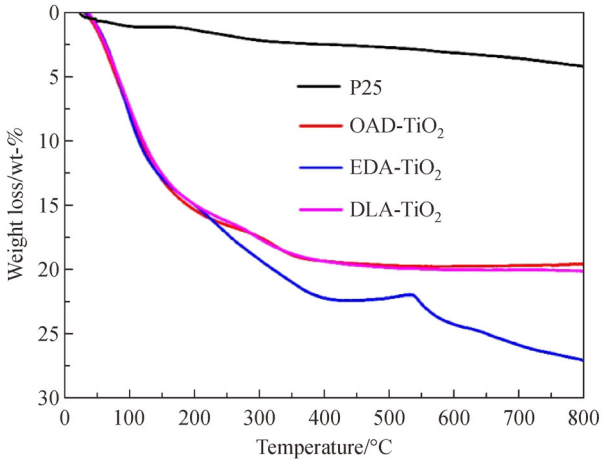

Fig. 2 TG spectra of the TiO_2 samples.

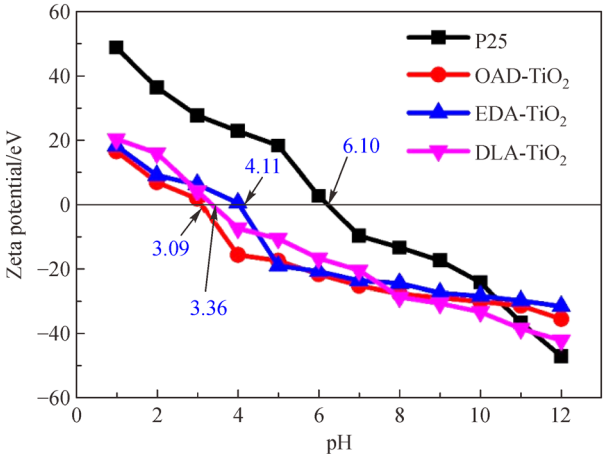

Fig. 3 Zeta potential of the TiO_2 samples. The numbers in blue mean isoelectronic point.

Table 2 Textural properties of the TiO_2 samples

Sample	S_{BET}/($m^2 \cdot g^{-1}$)	V_p/($cm^3 \cdot g^{-1}$)	R/nm
P25[a)]	48.48	0.258	1.07
OAD-TiO_2[b)]	30.47	0.043	2.88
EDA-TiO_2[c)]	25.56	0.188	8.92
DLA-TiO_2[d)]	401.26	0.366	1.83

a) P25: commercial bare TiO_2; b) OAD-TiO_2: oxalic acid modified TiO_2; c) EDA-TiO_2: ethylenediamine modified TiO_2; d) DLA-TiO_2: DL-alanine modified TiO_2.

explained by the fact that the S_{BET} of the TiO_2 samples greatly depends on the size of the aggregated TiO_2 particles, which is consistent with the result of SEM (Fig. S1). The V_p value also exhibits the similar variation tendency. The agglomeration of the organic components might cause the collapse of the porous structure and then led to the decrease of pore volume [28]. Furthermore, the hysteresis between the adsorption and desorption curves for OAD-TiO_2 illustrates the diffusion bottleneck in its tissue, probably owing to heterogeneous pore size. The pore radius of the samples calculated by the BJH method was in a narrow range of 1.0–9.0 nm, which indicates that all the TiO_2 samples have mesoporous and microporous structures. Such structures are attributed to the pores which are formed between TiO_2 particles [29]. From the result, it can be seen that the specific surface area of DLA-TiO_2 is much larger than that of OAD-TiO_2 and EDA-TiO_2, which is probably relative to the microporous structure [30]. These results indicate that the functional groups dramatically influence the surface texture of the functional TiO_2 samples.

3.2 Effect of pH

The initial solution pH is one of the most important factors for the adsorption process. The interaction between adsorbent and adsorbate could be effectively affected by the solution pH variation due to the change of surface characteristics for the adsorbent or the change of the form of adsorbates [31]. In this study, the ARG adsorption capacity onto the TiO_2 samples is dramatically influenced by the initial solution pH value (Fig. 4). The adsorption capacity is higher at low pH value and exhibits a sharp decline when the pH value is over the pH_{iep}. The positively charged surface of the samples and anionic nature of ARG indicate that the electrostatic interaction between ARG and the TiO_2 samples might play a meaningful role in adsorption process. However, it is obvious that P25 exhibits much lower adsorption capacity than other functional samples even it possesses a higher pH_{iep} value. This result suggests that electrostatic attraction is an important factor for the adsorption capacity of the modified samples but not the decisive reason for the enhanced adsorption performance.

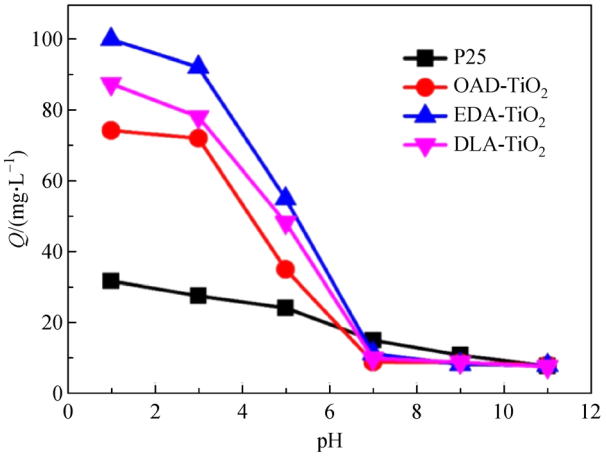

Fig. 4 Influence of the solution pH on the ARG adsorption onto the TiO_2 samples. Experimental conditions: initial ARG C_0 200 mg/L, dosage 2 g/L.

3.3 Adsorption kinetics

The adsorption kinetics of ARG onto the TiO_2 samples were studied by employing the initial ARG concentrations in the range of 100, 200 and 300 mg/L. The correlation between adsorption time and adsorption capacity of ARG at different initial concentrations are shown in the Fig. 5. As expected, the adsorption capacity increases as the time goes on and finally reaches a plateau, which indicates that the dynamic equilibrium between the adsorption and desorption was reached and no more molecules would be adsorbed even though the contact time prolonged. A very interesting result can be announced that the functional TiO_2 samples have a shorter equilibrium time than that of P25. The adsorption equilibrium of the functional TiO_2 samples can be reached within 20 min in all the used concentrations while the value for P25 is more than 40 min. This phenomenon indicates that the functional carboxyl and amino groups on the surface of the TiO_2 samples possesses a very obvious effect on the adsorption kinetics of ARG, which is consistent with the result of 'the reports' [32–34]. The adsorption kinetics of ARG onto P25 and the functional TiO_2 samples are also displayed in Fig. 5 and the corresponding parameters fitted by the pseudo-first-order and pseudo-second-order model are listed in Table 3. The adsorption behavior of ARG onto the four TiO_2 samples can be well described by the pseudo-second-order model (R^2 = 0.9919–0.9997). Furthermore, the calculated values of Q_e from the pseudo-second-order model are approximately equal to the experimental values (Q_{exp}). This indicates that the adsorption kinetics of ARG onto the TiO_2 samples corresponds well with the pseudo-second-order model and the adsorption process is mainly dominated by chemical reaction [35].

3.4 Adsorption isotherms

The adsorption isotherm study plays an important role in understanding the adsorption mechanism. The surface stacking of the adsorbates onto the adsorbent could be considered as a monolayer or multilayer state due to the isotherm models [36]. Herein, two common adsorption isotherm models, Freundlich and Langmuir models, were used to fit the experimental data at 25 °C. The corresponding experimental data and fitting curves of Langmuir and Freundlich models are shown in Fig. 6 (the isotherm fitting models at different temperature are shown in Fig. S3 (cf. ESM)), the fitting parameters are listed in

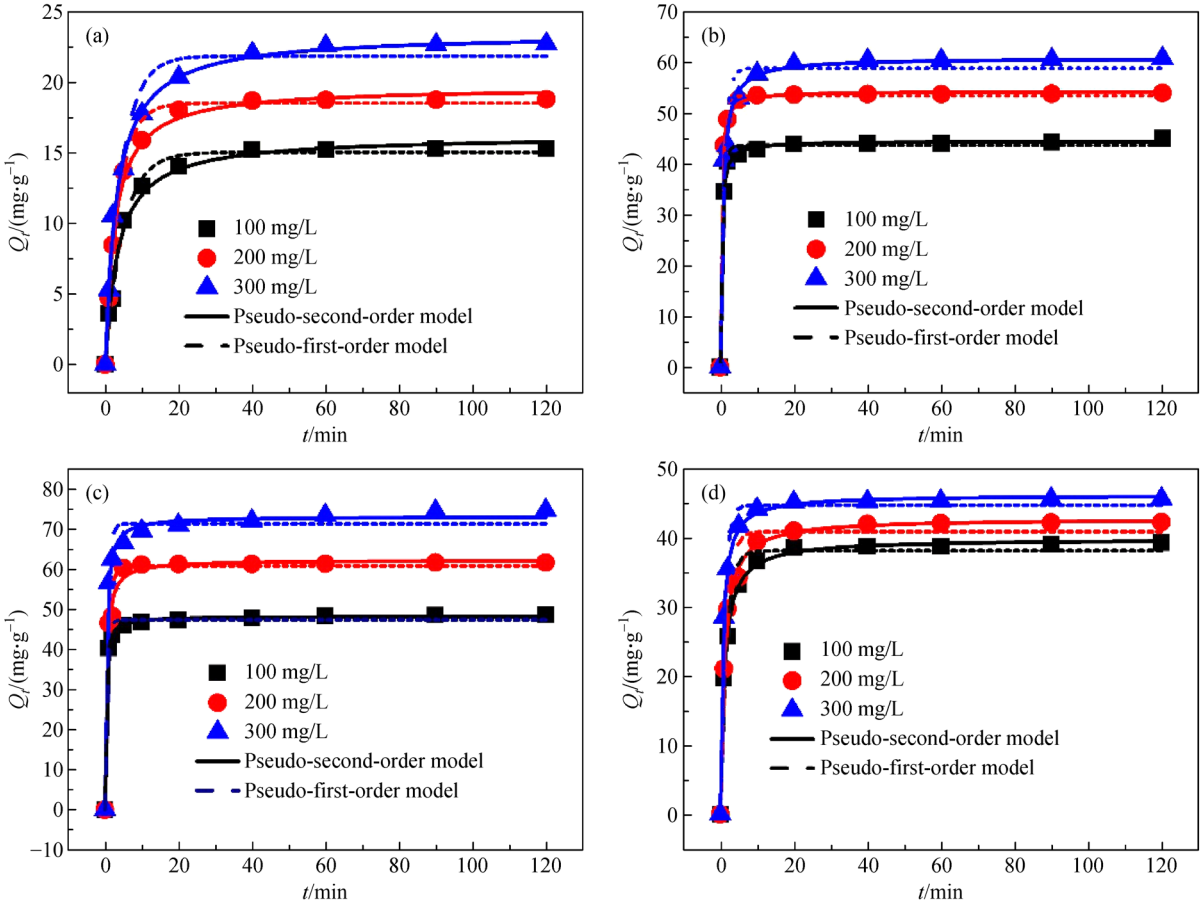

Fig. 5 Kinetics plots of ARG adsorbed onto (a) P25, (b) DLA-TiO_2, (c) EDA-TiO_2 and (d) OAD-TiO_2. Experimental conditions: initial C_0 100, 200, 300 mg/L, solution pH 3.0, dosage 2 g/L.

Table 3 Kinetics parameters for ARG adsorption at different initial concentrations

Sample	C_0 /(mg·L^{-1})	Q_{exp} /(mg·g^{-1})	Pseudo-first-order model			Pseudo-second-order model		
			k_1 /(L·min^{-1})	Q_e /(mg·g^{-1})	R^2	k_2 /(g·min^{-1}·mg^{-1})	Q_e /(mg·g^{-1})	R^2
P25[a)]	100	15.83	0.208	15.04	0.9894	0.018	16.22	0.9919
	200	18.82	0.273	18.53	0.9926	0.020	19.09	0.9947
	300	22.72	0.229	21.86	0.9714	0.014	23.15	0.9953
OAD-TiO_2[b)]	100	39.24	0.605	38.07	0.9832	0.024	39.78	0.9989
	200	42.17	0.640	40.81	0.9766	0.023	42.70	0.9975
	300	45.55	0.905	44.62	0.9904	0.036	46.08	0.9992
EDA-TiO_2[c)]	100	48.71	1.791	47.46	0.9923	0.101	48.28	0.9986
	200	61.78	1.195	60.93	0.9773	0.042	62.40	0.9996
	300	74.77	1.430	71.42	0.9810	0.043	73.21	0.9997
DLA-TiO_2[d)]	100	44.98	1.511	43.59	0.9952	0.084	44.45	0.9983
	200	53.93	1.610	53.33	0.9963	0.079	54.24	0.9994
	300	60.69	0.923	58.71	0.9637	0.027	60.77	0.9929

a) P25: commercial bare TiO_2; b) OAD-TiO_2: oxalic acid modified TiO_2; c) EDA-TiO_2: ethylenediamine modified TiO_2; d) DLA-TiO_2: DL-alanine modified TiO_2.

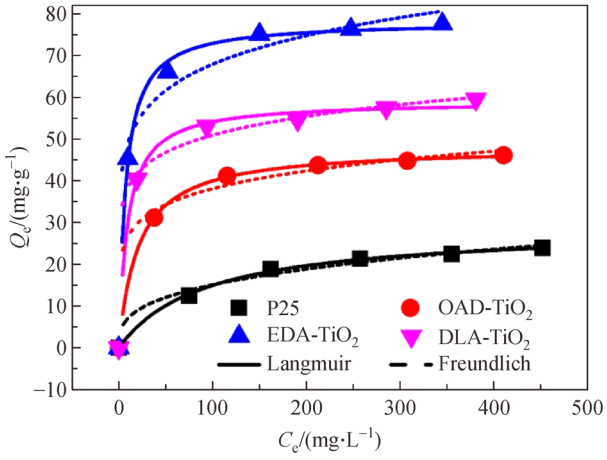

Fig. 6 Adsorption isotherms for ARG adsorbed onto the TiO_2 samples at 25 °C. Experimental conditions: initial ARG C_0 = 10–500 mg/L, solution pH 3.0, contact time 120 min.

Table 4 (the isotherm fitting parameters at different temperature are list in Table S1 (cf. ESM)). It is obvious that Langmuir model is more reasonable to describe the adsorption process of ARG onto P25 and the functional TiO_2 samples than Freundlich model according to the value of correlation coefficient (R^2), which significantly indicates that the adsorption sites on the surface of the TiO_2 samples are uniform and the adsorption of ARG onto the surface of the TiO_2 samples is monolayer [37]. The adsorption capacity of the functionalized TiO_2 samples for ARG obtained from the Langmuir model is larger than that of P25. Meanwhile, the adsorption capacity of DLA-TiO_2 is not higher than that of EDA-TiO_2, although DLA-TiO_2 has the larger specific surface area. The above result could be explained as follows: the partial specific surface area of DLA-TiO_2 comes from the microporous structure, while the ARG molecule is too large to enter the nanoscale pore structure for adsorption [38]. Moreover, the values of R_L are from 0.0143–0.1538 (in the range of 0–1.0), the values of 1/n are 0.122–0.323, which suggests that the adsorption

Table 4 Langmuir and Freundlich isotherm parameters for ARG adsorbed onto the TiO_2 samples

Samples	R_L	Langmuir model parameters			Freundlich model parameters		
		$Q_{m,cal}$/(mg·g^{-1})	K_L/(L·mg^{-1})	R^2	K_F/(mg·g^{-1})·(mg·L^{-1})$^{-n}$	1/n	R^2
P25[a)]	0.1538	28.78	0.011	0.9903	3.42	0.323	0.9293
OAD-TiO_2[b)]	0.0392	48.11	0.049	0.9969	18.86	0.153	0.9036
EDA-TiO_2[c)]	0.0143	78.15	0.138	0.9840	35.79	0.139	0.9078
DLA-TiO_2[d)]	0.0180	59.07	0.109	0.9567	29.01	0.122	0.9484

a) P25: commercial bare TiO_2; b) OAD-TiO_2: oxalic acid modified TiO_2; c) EDA-TiO_2: ethylenediamine modified TiO_2; d) DLA-TiO_2: DL-alanine modified TiO_2.

of ARG onto the functional TiO_2 surface is favorable. Furthermore, the values of R_L and $1/n$ for the functional TiO_2 samples are smaller than that of P25, indicating that the modified TiO_2 samples are prone to be the adsorption of ARG.

3.5 Regeneration performance of TiO_2 samples

To study the regeneration performance of the functional TiO_2 samples, NaOH solution (0.1 mol/L) and HNO_3 solution (0.1 mol/L) were employed as the desorption agent and the regeneration agent respectively because the adsorption capacity of ARG onto the TiO_2 samples is strongly pH dependent. The regenerated adsorbent (2 g/L) was reused to adsorb ARG (200 mg/L) at 25 °C, and the results of the adsorption capacity change versus the recycles are presented in Fig. 7. It is obvious that there is little loss of the adsorption capacity of the functional TiO_2 samples for ARG after five adsorption-desorption cycles. It is illustrated that the interactions between the fuanctional TiO_2 samples and ARG can be destroyed by dilute NaOH solution and the adsorption ability of the functional TiO_2 samples can be easily regenerated. The above results of the regeneration suggest functional TiO_2 is a promising adsorbent in the removal of ARG dye.

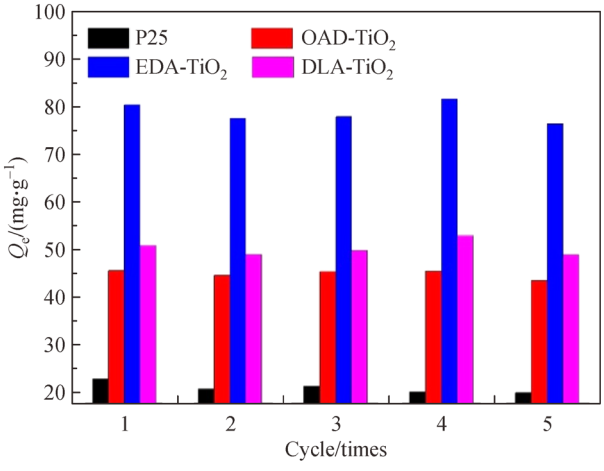

Fig. 7 Recycle performance of the TiO_2 samples with the initial concentrations of 200 mg/L of ARG, contact time of 120 min, at the temperature of 25 °C.

3.6 Adsorption mechanism

The result of the isotherm and kinetics experiments reveals the adsorption capacity of three functionalized TiO_2 samples were at the order of EDA (with two amino groups)-TiO_2 > DLA (with one amino group and one carboxyl group)-TiO_2 > OAD (with two carboxyl groups)-TiO_2, which is consistent with the result of the pH_{iep} test. OAD with two carboxyl groups in the molecule structure makes the TiO_2 negatively charged easily. With the amino group introduced, the pH_{iep} of samples is much larger than that of OAD-TiO_2 because the amino group is easy to protonate so that it carries more positive charges on the surface of TiO_2. Meanwhile, ARG is a typical anionic dye, which is easily adsorbed by the adsorbent with more positive charge. Therefore, the adsorption capacity of the functional TiO_2 samples is in accordance with the above order. However, it is also obvious that the adsorption capacity of P25 is less than all of the functional samples though the pH_{iep} of P25 is largest in the samples. This result illustrate that though electrostatic attraction makes contribution to the impact for the adsorption capacity, there are also some more important factors for the adsorption mechanisms. Therefore, the FTIR analysis were used to find more precise conclusion.

The FTIR spectra of the three TiO_2 samples before and after the adsorption of ARG are presented in Fig. 8. It is illustrated that the obvious shifting of peaks occurred, and some new peaks related to ARG appeared after adsorption process. In detail, the peaks of 1496 ($\nu_{C=C}$ for benzenoid rings in ARG molecule), 1218 ($\nu_{=N-C}$ connect with phenyl), and 1045 cm^{-1} ($\nu_{-S=O}$ for the $-SO_3^-$ in ARG molecule) [39,40] appeared after adsorbed by all the three functional TiO_2 samples, respectively. These peaks illustrate that ARG was successfully adsorbed onto the functional TiO_2 samples. Meanwhile, the peak 1690 cm^{-1} ($\nu_{C=O}$) in OAD-TiO_2 and the peak 1510 cm^{-1} (ν_{N-H} in the secondary amino) in DLA-TiO_2 and EDA-TiO_2 disappeared, which indicates that there are interactions between ARG and the carboxyl or amino groups in the TiO_2 samples during the adsorption. In addition, the adsorption performance of EDA-TiO_2 is better than DLA-TiO_2 and OAD-TiO_2 according to the experimental data. The above results demonstrate that functional groups, especially amino groups play an important role in the adsorption of ARG, which could also account for the poor adsorption capacity of P25.

According to the previous analysis and literatures [41,42], the interaction between ARG and functional groups especially amino group made the main contribution to the adsorption of organic dye onto the modified TiO_2 samples, and electrostatic interaction is also involved in this process. In the desorption process, these interactions could be destroyed easily in the alkaline solution, which results in the desorption of ARG from the modified TiO_2 samples.

4 Conclusions

The interfacial functionalized TiO_2 samples with carboxyl and amino groups were successfully prepared at lower temperature by using hydrolysis method and exhibited an enhanced adsorption performance for removal of anionic dye ARG from aqueous solution. The carboxyl group combined into the TiO_2 with bridging and chelating

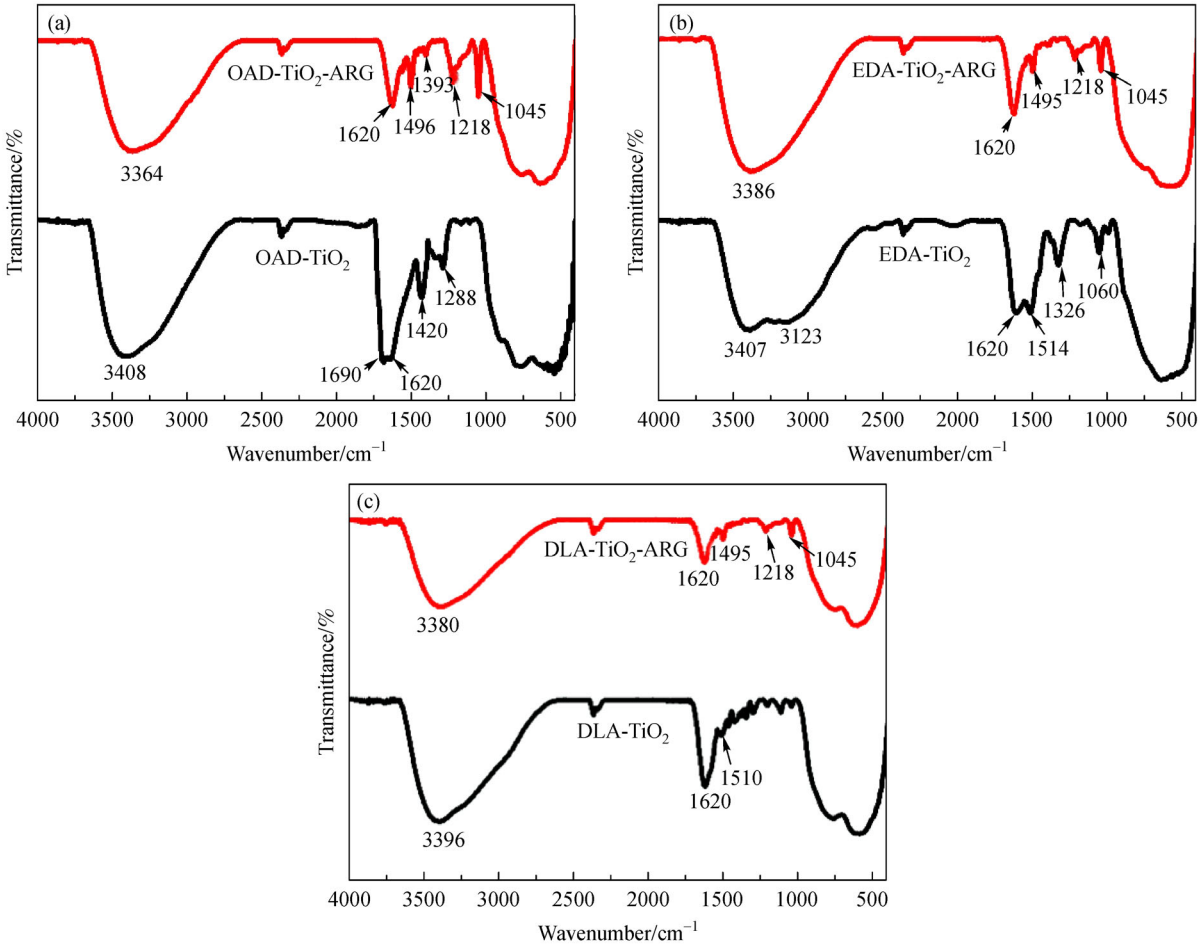

Fig. 8 FTIR spectra of (a) OAD-TiO_2, (b) EDA-TiO_2, and (c) DLA-TiO_2 before and after adsorption of ARG. The data before and after adsorption of ARG are represented by black and red curves, respectively.

structure, while the amino group anchored into the TiO_2 with hydrogen bonding. The introduction of carboxyl and amino groups had a significant effect on the physicochemical properties of the functional TiO_2, such as surface charge, thermal stability, surface texture, and further influenced the adsorption performance of the functionalized TiO_2 samples for anionic dye ARG. The functionalized TiO_2 displays a higher adsorption capacity, faster adsorption rate and better regeneration than that of P25. The EDA modified TiO_2 has the maximum adsorption capacity for ARG as 78.15 mg/g, while that of DLA-TiO_2 is 59.07 mg/g, and the OAD-TiO_2 is 48.11 mg/g. We find that the main adsorption mechanism is the interaction between ARG and amino groups or carboxyl groups and the surface charge is also related to this process. In summary, the carboxyl and amino groups in the functional TiO_2 have dramatic influence on the physicochemical properties of TiO_2, and further impact the adsorption performance. This discovery could provide a powerful proof for the design of some specific adsorbent for organic dyes removal.

Acknowledgements The authors gratefully acknowledge the Shaanxi Key research and development projects, China (Grant No. 2017SF-386), the Fundamental Research Funds for the Central Universities of China and the Key Industrial Project in Xianyang City, Shaanxi, China (Grant No. 2018k02-10).

Electronic Supplementary Material Supplementary material is available in the online version of this article at https://doi.org/10.1007/s11705-020-1978-x and is accessible for authorized users.

References

1. Park H, Kim H I, Moon G H, Choi W. Photoinduced charge transfer processes in solar photocatalysis based on modified TiO_2. Energy & Environmental Science, 2016, 9(2): 411–433
2. Nakata K, Fujishima A. TiO_2 photocatalysis: design and applications. Journal of Photochemistry and Photobiology C, Photochemistry Reviews, 2012, 13(3): 169–189
3. Schneider J, Matsuoka M, Takeuchi M, Zhang J, Horiuchi Y, Anpo M, Bahnemann D W. Understanding TiO_2 photocatalysis: mechanisms and materials. Chemical Reviews, 2014, 114(19): 9919–9986
4. Xu H, Ouyang S, Liu L, Reunchan P, Umezawa N, Ye J. Recent

advances in TiO_2-based photocatalysis. Journal of Materials Chemistry. A, Materials for Energy and Sustainability, 2014, 2 (32): 12642–12661

5. Prieto Rodriguez L, Miralles Cuevas S, Oller I, Aguera A, Li Puma G, Malato S. Treatment of emerging contaminants in wastewater treatment plants (WWTP) effluents by solar photocatalysis using low TiO_2 concentrations. Journal of Hazardous Materials, 2012, 211: 131–137
6. Marinho B A, Cristóvão R O, Djellabi R, Loureiro J M, Boaventura R A, Vilar V J P. Photocatalytic reduction of Cr(VI) over TiO_2-coated cellulose acetate monolithic structures using solar light. Applied Catalysis B: Environmental, 2017, 203: 18–30
7. Choi Y, Koo M S, Bokare A D, Kim D H, Bahnemann D W, Choi W. Sequential process combination of photocatalytic oxidation and dark reduction for the removal of organic pollutants and Cr(VI) using Ag/TiO_2. Environmental Science & Technology, 2017, 51(7): 3973–3981
8. Xiong L, Sun W, Yang Y, Chen C, Ni J. Heterogeneous photocatalysis of methylene blue over titanate nanotubes: effect of adsorption. Journal of Colloid and Interface Science, 2011, 356(1): 211–216
9. Nguyen-Phan T D, Song M B, Shin E W. Removal efficiency of gaseous benzene using lanthanide-doped mesoporous titania. Journal of Hazardous Materials, 2009, 167(1-3): 75–81
10. Zhang L, Cole J M, Dai C. Variation in optoelectronic properties of azo dye-sensitized TiO_2 semiconductor interfaces with different adsorption anchors: carboxylate, sulfonate, hydroxyl and pyridyl groups. ACS Applied Materials & Interfaces, 2014, 6(10): 7535–7546
11. Kim B, Park S W, Kim J Y, Yoo K, Lee J A, Lee M W, Lee D K, Kim J Y, Kim B, Kim H, Han S, Son H J, Ko M J. Rapid dye adsorption via surface modification of TiO_2 photoanodes for dye-sensitized solar cells. ACS Applied Materials & Interfaces, 2013, 5(11): 5201–5207
12. Natarajan T S, Bajaj H C, Tayade R J. Preferential adsorption behavior of methylene blue dye onto surface hydroxyl group enriched TiO_2 nanotube and its photocatalytic regeneration. Journal of Colloid and Interface Science, 2014, 433: 104–114
13. Sugita T, Kobayashi K I, Kobayashi K, Yamazaki T, Fujii K, Itabashi H, Mori M. Enhanced aqueous adsorption and photo-decomposition of anionic organic target by amino group-modified TiO_2 as anionic adsorptive photocatalyst. Journal of Photochemistry and Photobiology A Chemistry, 2018, 356: 71–80
14. Baig M I, Ingole P G, Choi W K, Park S R, Kang E C, Lee H K. Development of carboxylated TiO_2 incorporated thin film nano-composite hollow fiber membranes for flue gas dehydration. Journal of Membrane Science, 2016, 514: 622–635
15. Nguyen-Le M T, Lee B K. High temperature synthesis of interfacial functionalized carboxylate mesoporous TiO_2 for effective adsorption of cationic dyes. Chemical Engineering Journal, 2015, 281: 20–33
16. Liu J M, Han L, An N, Xing L, Ma H Y, Cheng L, Yang J C, Zhang Q C. Enhanced visible-light photocatalytic activity of carbonate-doped anatase TiO_2 based on the electron-withdrawing bidentate carboxylate linkage. Applied Catalysis B: Environmental, 2017, 202: 642–652
17. Wang J, Yang G, Chen J, Liu Y, Wang Y, Lao C Y, Xi K, Yang D, Harris C J, Yan W, Ding S, Kumar R V. Flexible and High-loading lithium-sulfur batteries enabled by integrated three-in-one fibrous membranes. Advanced Energy Materials, 2019, 9(38): 1902001
18. Weng Y, Li L, Liu Y, Wang L, Yang G. Surface-binding forms of carboxylic groups on nanoparticulate TiO_2 surface studied by the interface-sensitive transient triplet-state molecular probe. Journal of Physical Chemistry B, 2003, 107(18): 4356–4363
19. Karapati S, Giannakopoulou T, Todorova N, Boukos N, Dimotikali D, Trapalis C. Eco-efficient TiO_2 modification for air pollutants oxidation. Applied Catalysis B: Environmental, 2015, 176-177: 578–585
20. Mallakpour S, Nikkhoo E. Surface modification of nano-TiO_2 with trimellitylimido-amino acid-based diacids for preventing aggregation of nanoparticles. Advanced Powder Technology, 2014, 25(1): 348–353
21. Shi B, Zhao C, Ji Y, Shi J, Yang H. Promotion effect of PANI on Fe-PANI/zeolite as an active and recyclable Fenton-like catalyst under near-neutral condition. Applied Surface Science, 2020, 508: 145298
22. Li X, Wang D, Cheng G, Luo Q, An J, Wang Y. Preparation of polyaniline-modified TiO_2 nanoparticles and their photocatalytic activity under visible light illumination. Applied Catalysis B: Environmental, 2008, 81(3-4): 267–273
23. Janković I A, Šaponjić Z V, Čomor M I, Nedeljković J M. Surface modification of colloidal TiO_2 nanoparticles with bidentate benzene derivatives. Journal of Physical Chemistry C, 2009, 113(29): 12645–12652
24. Duckworth O W, Martin S T. Surface complexation and dissolution of hematite by C1–C6 dicarboxylic acids at pH = 5.0. Geochimica et Cosmochimica Acta, 2001, 65(23): 4289–4301
25. Filius J D, Hiemstra T, Van Riemsdijk W H. Adsorption of small weak organic acids on goethite: modeling of mechanisms. Journal of Colloid and Interface Science, 1997, 195(2): 368–380
26. Crake A, Christoforidis K C, Godin R, Moss B, Kafizas A, Zafeiratos S, Durrant J R, Petit C. Titanium dioxide/carbon nitride nanosheet nanocomposites for gas phase CO_2 photoreduction under UV-visible irradiation. Applied Catalysis B: Environmental, 2019, 242: 369–378
27. Feng J, Zhu J, Lv W, Li J, Yan W. Effect of hydroxyl group of carboxylic acids on the adsorption of acid red G and methylene blue on TiO_2. Chemical Engineering Journal, 2015, 269: 316–322
28. Yu J C, Yu J G, Ho W K, Jiang Z T, Zhang L Z. Effects of F-doping on the photocatalytic activity and microstructures of nanocrystalline TiO_2 powders. Chemistry of Materials, 2002, 14(9): 3808–3816
29. Yu J C, Yu J G, Ho W K, Zhang L Z. Preparation of highly photocatalytic active nano-sized TiO_2 particles via ultrasonic irradiation. Chemical Communications, 2001, 19(19): 1942–1943
30. Lyu W, Wu J M, Zhang W L, Liu Y P, Yu M T, Zhao Y F, Feng J T, Yan W. Easy separated 3D hierarchical coral-like magnetic polyaniline adsorbent with enhanced performance in adsorption and reduction of Cr(VI) and immobilization of Cr(III). Chemical Engineering Journal, 2019, 363: 107–119
31. Moreno-Castilla C. Adsorption of organic molecules from aqueous solutions on carbon materials. Carbon, 2004, 42(1): 83–94
32. Shayegan Z, Haghighat F, Lee C S, Bahloul A, Huard M. Effect of

surface fluorination of P25-TiO_2 on adsorption of indoor environment volatile organic compounds. Chemical Engineering Journal, 2018, 346: 578–589

33. Li S, Fang L, Ye M, Zhang Y. Enhanced adsorption of norfloxacin on modified TiO_2 particles prepared via surface molecular imprinting technique. Desalination and Water Treatment, 2016, 57: 408–418
34. Leong S, Li D, Hapgood K, Zhang X W, Wang H T. $Ni(OH)_2$ decorated rutile TiO_2 for efficient removal of tetracycline from wastewater. Applied Catalysis B: Environmental, 2016, 198: 224–233
35. Wang L, Wang J, Wang Z, He C, Lyu W, Yan W, Yang L. Enhanced antimonate (Sb(V)) removal from aqueous solution by La-doped magnetic biochars. Chemical Engineering Journal, 2018, 354: 623–632
36. Srinivasan A, Viraraghavan T. Decolorization of dye wastewaters by biosorbents: a review. Journal of Environmental Management, 2010, 91(10): 1915–1929
37. Zhang W L, Fu R, Wang L, Zhu J W, Feng J T, Yan W. Rapid removal of ammonia nitrogen in low-concentration from wastewater by amorphous sodium titanate nano-particles. Science of the Total Environment, 2019, 668: 815–824
38. Suresh Kumar P, Korving L, Keesman K J, van Loosdrecht M, Witkamp G. Effect of pore size distribution and particle size of porous metal oxides on phosphate adsorption capacity and kinetics. Chemical Engineering Journal, 2019, 358: 160–169
39. Han X X, Zhu G Q, Ding Y X, Miao Y L, Wang K W, Zhang H J, Wang Y, Liu S B. Selective catalytic synthesis of glycerol monolaurate over silica gel-based sulfonic acid functionalized ionic liquid catalysts. Chemical Engineering Journal, 2019, 359: 733–745
40. Han X, Yan W, Hung C T, He Y, Wu P H, Liu L L, Huang S J, Liu S B. Transesterification of soybean oil to biodiesel by tin-based Brønsted-Lewis acidic ionic liquid catalysts. Korean Journal of Chemical Engineering, 2016, 33(7): 2063–2072
41. Zhang X, Bai R. Adsorption behavior of humic acid onto polypyrrole-coated nylon 6,6-granules. Journal of Materials Chemistry, 2002, 12(9): 2733–2739
42. Li J, Zhang Q, Feng J, Yan W. Synthesis of PPy-modified TiO_2 composite in H_2SO_4 solution and its novel adsorption characteristics for organic dyes. Chemical Engineering Journal, 2013, 225: 766–775